

Lawrence Berkeley National Laboratory

Lawrence Berkeley National Laboratory

Title

The Methanosarcina barkeri genome: comparative analysis with Methanosarcina acetivorans and Methanosarcina mazei reveals extensive rearrangement within methanosarcinal genomes

Permalink

<https://escholarship.org/uc/item/3g16p0m7>

Authors

Maeder, Dennis L.
Anderson, Iain
Brettin, Thomas S.
et al.

Publication Date

2006-05-19

Peer reviewed



ERNEST ORLANDO LAWRENCE BERKELEY NATIONAL LABORATORY

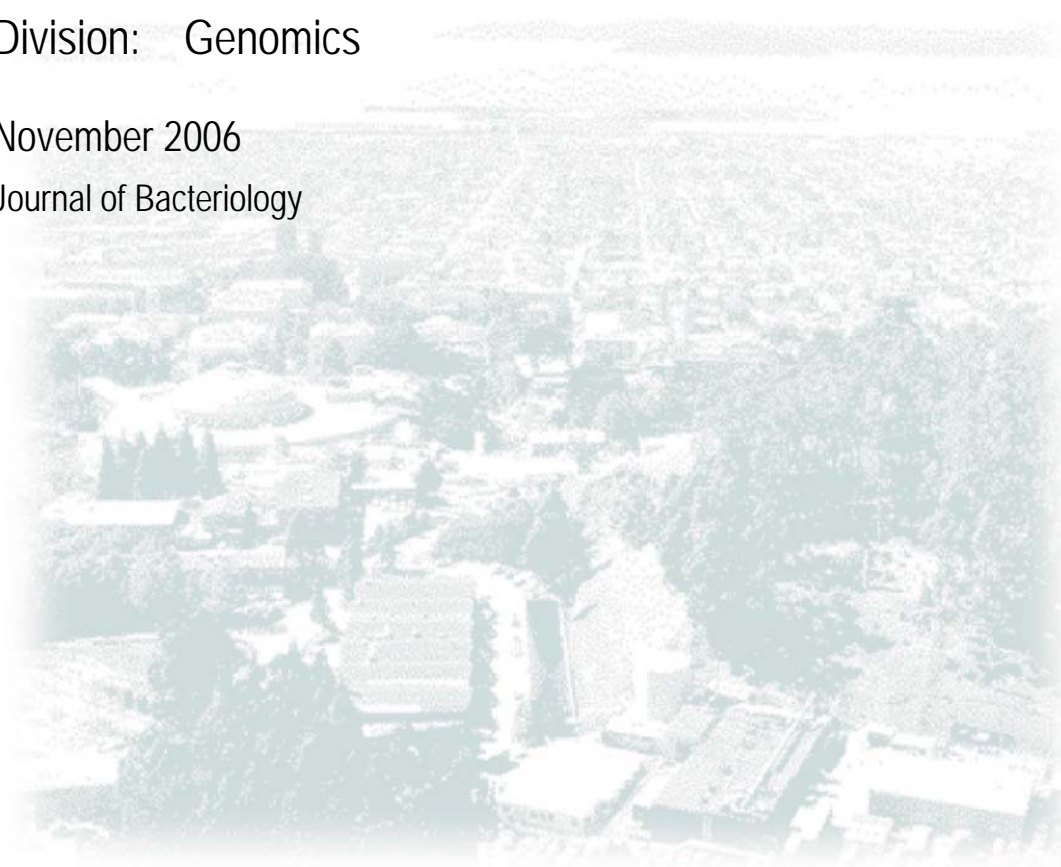
Title: The *Methanosarcina barkeri* genome: comparative analysis with *Methanosarcina acetivorans* and *Methanosarcina mazei* reveals extensive rearrangement within methanosarcinal genomes

Author(s): Dennis L. Maeder, Iain Anderson, et al

Division: Genomics

November 2006

Journal of Bacteriology



1

2 **The *Methanosarcina barkeri* genome: comparative analysis**
3 **with *Methanosarcina acetivorans* and *Methanosarcina mazei***
4 **reveals extensive rearrangement within methanosarcinal**
5 **genomes**

6

7

8

9 Dennis L. Maeder*, Iain Anderson†, Thomas S. Brettin†, David C. Bruce†, Paul Gilna†,

10 Cliff S. Han†, Alla Lapidus†, William W. Metcalf‡, Elizabeth Saunders†, Roxanne

11 Tapia†, and Kevin R. Sowers*.

12

13 * *University of Maryland Biotechnology Institute, Center of Marine Biotechnology,*
14 *Columbus Center, Suite 236, 701 E. Pratt St., Baltimore, Maryland 21202, USA*

15 † *Microbial Genomics, DOE Joint Genome Institute, 2800 Mitchell Drive, B400, Walnut*
16 *Creek, CA 94598, USA*

17 ‡ *University of Illinois, Department of Microbiology, B103 Chemical and Life Sciences*
18 *Laboratory, 601 S. Goodwin Avenue, Urbana, Illinois 61801, USA*

19

20 Running title: Comparative analysis of three methanosarcinal genomes

21

22 Keywords: *Methanosarcina barkeri*, archaeal genome, methanogenic Archaea

23 **ABSTRACT**

24

25 We report here a comparative analysis of the genome sequence of
26 *Methanosarcina barkeri* with those of *Methanosarcina acetivorans* and
27 *Methanosarcina mazei*. All three genomes share a conserved double origin of
28 replication and many gene clusters. *M. barkeri* is distinguished by having an
29 organization that is well conserved with respect to the other *Methanosarcinae* in the
30 region proximal to the origin of replication with interspecies gene similarities as high as
31 95%. However it is disordered and marked by increased transposase frequency and
32 decreased gene synteny and gene density in the proximal semi-genome. Of the 3680
33 open reading frames in *M. barkeri*, 678 had paralogs with better than 80% similarity to
34 both *M. acetivorans* and *M. mazei* while 128 nonhypothetical orfs were unique (non-
35 paralogous) amongst these species including a complete formate dehydrogenase
36 operon, two genes required for N-acetylmuramic acid synthesis, a 14 gene gas vesicle
37 cluster and a bacterial P450-specific ferredoxin reductase cluster not previously
38 observed or characterized in this genus. A cryptic 36 kbp plasmid sequence was
39 detected in *M. barkeri* that contains an *orc1* gene flanked by a presumptive origin of
40 replication consisting of 38 tandem repeats of a 143 nt motif. Three-way comparison of
41 these genomes reveals differing mechanisms for the accrual of changes. Elongation of
42 the large *M. acetivorans* is the result of multiple gene-scale insertions and duplications
43 uniformly distributed in that genome, while *M. barkeri* is characterized by localized
44 inversions associated with the loss of gene content. In contrast, the relatively short *M.*
45 *mazei* most closely approximates the ancestral organizational state.

46 INTRODUCTION

47
48 Biological methanogenesis by the methane-producing Archaea has a significant
49 role in the global carbon cycle. This process is one of several anaerobic degradative
50 processes that complement aerobic degradation by utilizing alternative electron
51 acceptors in habitats where O₂ is not available (Sowers 2004). The efficiency of this
52 microbial process is directly dependent upon the interaction of three metabolically
53 distinct groups of microorganisms: the fermentative and acetogenic Bacteria and the
54 methanogenic Archaea. The methanogenic Archaea have two pivotal roles in
55 methanogenic consortia (Lovley and Klug 1982). By consuming hydrogen for
56 methanogenesis and effectively lowering its partial pressure by the process of inter-
57 species hydrogen exchange, the methanogens provide a thermodynamically favorable
58 environment for the fermentative and acetogenic species to utilize protons as electron
59 acceptors. This interaction enables fermentors to conserve more energy by producing a
60 more oxidized product, acetate, which is a substrate for methanogenesis. The second
61 role of the methanogens is the dismutation of acetate, which accounts for 70% of the
62 global methane produced by biological methane production. The net effect of inter-
63 species hydrogen exchange is the diversion of protons to hydrogen and carbon to
64 acetate, which ultimately yields methane and carbon dioxide via methanogenesis.

65 The genus *Methanosarcina* includes the most metabolically diverse species of
66 methanogens. Whereas most methanogenic species grow by obligate CO₂ reduction
67 with H₂, methyl reduction with H₂, aceticlastic dismutation of acetate or methylotrophic

68 catabolism of methanol, methylated amines, and dimethylsulfide, most *Methanosarcina*
69 spp. grow by all four catabolic pathways (Welander and Metcalf 2005).
70 *Methanosarcina acetivorans* was recently reported also to grow non-methanogenically
71 with CO (Rother and Metcalf 2004). In addition to their appetency for all known
72 methanogenic substrates most *Methanosarcina* spp. can grow in a minimal mineral
73 medium and fix molecular nitrogen (Bomar and Knoll 1985; Lobo and Zinder 1988).
74 They also adapt to intracellular solute concentrations ranging from freshwater to three
75 times that found in seawater (Sowers 1995) by osmoregulatory mechanisms that enable
76 them to synthesize or accumulate osmoprotectants and modify their outer cell envelope
77 (Sowers et al. 1993). This metabolic diversity is reflected in the relatively large genome
78 sizes of *Methanosarcina acetivorans* (5.8 Mb) and *Methanosarcina mazei* (4.1 Mb)
79 genomes and the relatively large number of number of putative coding sequences,
80 4,524 and 3,371 respectively, compared with other methanogenic Archaea
81 (Deppenmeier et al. 2002; Galagan et al. 2002). The adaptive success of these species
82 is further evident by the occurrence of multiple orthologs in the genomes including
83 multiple catabolic methyltransferases and carbon monoxide dehydrogenases, all three
84 known types of nitrogenases, and all four known chaperoning systems (Conway de
85 Macario et al. 2003; Deppenmeier et al. 2002; Galagan et al. 2002).

86 *Methanosarcina barkeri* Fusaro was isolated from sediment from Lago del
87 Fusaro, a freshwater coastal lagoon west of Naples, Italy (Kandler and Hippe 1977).
88 This isolate utilizes all three catabolic pathways and exhibits a dichotomous
89 morphology. When grown on freshwater medium this species grows as large
90 multicellular aggregates imbedded in a heteropolysaccharide matrix (Figure 1)

91 composed primarily of D-galactosamine and D-glucuronic acid, termed
92 methanochondroitin (Kreisl and Kandler 1986), whereas in marine medium these
93 species grow as individual cells surrounded only by an S-layer (Sowers 1995). This
94 isolate has been one of the most frequently studied methanosarcinal strains for the
95 physiology, biochemistry and bioenergetics of methanogenesis (Sowers 2004). The
96 development of a tractable methanosarcinal gene transfer system has led to a number
97 of recent reports on the mechanisms of methanogenesis using genetic approaches
98 (Rother and Metcalf 2005).

99 Herein we describe the genome of *M. barkeri*, which represents the third
100 methanosarcinal genome sequenced. In addition to comparison of the genome
101 annotation, this is the first three-way analysis of the complete genomes of closely
102 related species in the methanogenic *Euryarchaeota*. Results reveal extensive gene
103 rearrangements in *M. barkeri* relative to *M. acetivorans* and *M. mazei* and high degree
104 of conservation within the fragments providing insight into the mechanisms of structural
105 modification and the functional organization of the methanosarcinal genome.

106 **MATERIALS AND METHODS**

107

108 **Growth conditions**

109 The source for *Methanosarcina barkeri* Fusaro (=DSM 804) was described
110 previously (Metcalf et al. 1996). *M. barkeri* was grown in F-medium (Sowers 1995) with
111 0.1 M trimethylamine, Where described growth was tested with 0.1 M sodium formate or
112 with a headspace of 200 kPa H₂-CO₂ (80:20) substituted for trimethylamine. Cultures

113 were incubated statically at 35 °C in the dark. Growth was monitored by measuring the
114 optical density at 550 nm with a Spectronic 21 and by measuring methanogenesis by
115 gas chromatography as described previously (Sowers et al. 1993; Sowers and Ferry
116 1983).

117 Genome sequencing, assembly and finishing

118 Genomic DNA was isolated from *M. barkeri* Fusaro as described previously
119 (Boccazzi et al. 2000). The genome of *M. barkeri* was sequenced at the Joint Genome
120 Institute (JGI) using a combination of 3 kb, 8 kb and 40 kb (fosmid) DNA libraries. All
121 general aspects of library construction and sequencing performed at the JGI can be
122 found at <http://www.jgi.doe.gov/>. Draft assemblies were based on 89216 total reads.
123 All three libraries provided 13x coverage of the genome. The Phred/Phrap/Consed
124 software package (<http://www.phrap.com>) was used for sequence assembly and quality
125 assessment (Ewing and Green 1998; Ewing et al. 1998; Gordon et al. 1998). After the
126 shotgun stage, reads were assembled with parallel phrap (High Performance Software,
127 LLC). Possible mis-assemblies were corrected with Dupfinisher (unpublished, C. Han)
128 or transposon bombing of bridging clones (Epicentre Biotechnologies, Madison, WI).
129 Gaps between contigs were closed by editing in Consed, custom primer walk or PCR
130 amplification (Roche Applied Science, Indianapolis, IN). A total of 2389 additional
131 reactions were necessary to close gaps and to raise the quality of the finished
132 sequence. The completed genome sequences of *M. barkeri* contains 85812 reads,
133 achieving an average of 12-fold sequence coverage per base with an error rate less
134 than 1 in 100,000. The sequences of *M. barkeri*, including a chromosome and a

135 plasmid, can be accessed using the GenBank accession numbers CP000099 and
136 CP000098 or from the JGI IMG site (<http://img.jgi.doe.gov>) as taxon ID 623520000.

137 Annotation and analysis

138 Genes were predicted with a combination of Glimmer and Critica (Badger and
139 Olsen 1999; Delcher et al. 1999). These gene predictions were then run through a
140 pipeline that identifies gene overlaps, missed genes, and incorrect start sites (Markowitz
141 et al. 2006). The gene predictions were then manually curated. Functional predictions
142 were generated automatically based on presence of hits to COGs (Tatusov et al. 2003),
143 Pfam (Bateman et al. 2000), and Interpro (Mulder et al. 2005) families.

144 Whole genome alignment and analysis

145 Chromosome sequences (Table 1) in fasta format were used to build single
146 sequence blast databases, which served as the subject sequences for comprehensive
147 WuBlast (Gish, W., 1996-2004, <http://blast.wustl.edu>) blastn and tblastx paired
148 comparisons both as whole sequences and as segmented comparisons using the
149 following parameters: span2, noseqs, filter=none, hspmax =10000, gspmax=10000.
150 Similarly all CDS sequence features were built into databases and blasted to generate a
151 comprehensive set of pairwise comparisons. Blastn outputs were captured into a
152 database of HSP features cross referenced to a sequence and sequence feature
153 database. Outputs were also directly parsed by Cross (Maeder, D., 1998-2006,
154 <http://bigm.umbi.umd.edu/materials/software/Cross.pub/>) for display and interactive
155 examination of comparative features.

156 The paired comparison database, GRIT, runs under the database manager
157 MySQL (MySQL AB) and consists of source, feature, fragment and link tables. The
158 feature table was populated with predicted gene product features derived from
159 GenBank or JGI (Table 1) with a foreign key pointing to a source table. The link table
160 contains blastn HSP scores and identities with foreign keys pointing to entries in the
161 fragment table, which contains positional information about HSPs with a foreign key
162 pointing to the feature from which it was derived. This schema (Figure 2) allows the
163 construction of a SQL query that directly and rapidly retrieves sets of features, which
164 are either unique within a set of source chromosomes or describes a set of genes
165 common at an arbitrary level of similarity between two or more sources. Blastn
166 comparisons facilitate measurement of significant similarity in homologs of closely
167 related organisms and manage non-coding sequences; tblastx or blastx comparisons
168 are similarly applicable for comparison of less closely related sequences. Washu blastn
169 was used with the parameters: span2, filter=none, hspmax =10000, gspmax=10000,
170 and was wrapped in a perl script for automatic iteration through multiple pair-wise
171 blasts. Output data were then parsed and HSPs stored in GRIT. A web interface to the
172 queries and databases is available at (<http://bigm.umbi.umd.edu/dat/genome/>) and will
173 be elaborated elsewhere.

174 Cumulative skew analysis was performed using skew (Maeder, 2001,
175 <http://bigm.umbi.umd.edu/materials/software/skew/>) which implements the algorithm of
176 Grigoriev (Grigoriev 1998). Repeat analysis emerged directly from unfiltered blast and
177 was confirmed using Mummer (Delcher et al. 1999). Putative origins of replication were

178 explored by examining regions with locally separated inverted repeats in close upstream
179 proximity to the *orc1/cdc6* genes.

180 Chromosomal sequence similarity was calculated as a distance derived from
181 blastn comparisons in the GRIT database using a perl script cross match.pl which
182 generates distance matrices in mega2 format based on equation 1, where n is the
183 length of the genome and HSP.ID is the maximal fractional identity at position n of
184 sequence x where HSP.ID exceeds a threshold of e.g. 0.67. The mean distance D for
185 both axes is calculated for both sequence axes by the equation:

$$186 \quad D_x = 1 - \sum_1^n (MAX(HSP.ID_n)) / n \quad (1)$$

187 This measure of distance is comparable with hybridization techniques as it yields a
188 fractional nucleotide similarity between organisms which considers stringency.

189 Synteny of any gene was measured by comparing the order of the gene's left
190 and right neighbors with those of their best matched paralogous genes in the
191 comparable genome. Downstream synteny is expressed as the ratio of the ordinal
192 distance between a gene, G, and its downstream neighbor, R, (which is always 1) and
193 the distance between a corresponding paralogous gene G' and the paralog of R, R'.

194 This may be calculated as:

$$195 \quad SI = 1 / abs(R' - G') \quad (2)$$

196 with $0 < SI \leq 1$. Cumulative deviations from the mean of SI were calculated for
197 intelligible display. Intergenic interval was calculated in the same manner.

198 **Microscopy**

199 For thin-section electron micrographs, cells were fixed with 2% glutaraldehyde
200 and 2% osmium tetroxide, and dehydrated in a graded series of ethanol mixtures. Cells
201 were embedded and sectioned in Epon resin, then post-stained with uranyl acetate and
202 lead citrate as described previously (Sowers and Ferry 1983). A Joel JEM-1200 EX II
203 transmission electron microscope at 80 kV was used to generate thin-section
204 micrographs.

205 **RESULTS & DISCUSSION**

206
207

208 The genome of *Methanosarcina barkeri* was sequenced using a combination of
209 whole genome shotgun and directed finishing as described in Methods. The genome
210 consists of a circular chromosome of 4,837,408 base pairs (bp) and a 36,358 bp
211 extrachromosomal element (Table 1). The *M. barkeri* genome, which is intermediate in
212 size between *Methanosarcina acetivorans* (5.8 mb) and *Methanosarcina mazei* (4.1
213 mb), is the second largest genome among the Archaea. The extrachromosomal
214 element is 6.7 times larger than the only other methanosarcinal extrachromosomal
215 element, plasmid pC2A, from *M. acetivorans* (Metcalf et al. 1997).

216 ***Methanosarcina barkeri* chromosome structure and content**

217
218

219 A total of 3680 putative protein coding genes longer than 200 bp were identified
219 (Table 1), which together cover 70% of the genome. The average protein coding region
220 of *M. barkeri* at 921 bp is within 2% of *M. acetivorans* and *M. mazei* while its average
221 intergenic region at 393 bp is considerably larger than those of *M. acetivorans* (328 bp)

222 and *M. mazei* (303 bp). A further 73 RNA features were identified including 3 sets of
223 ribosomal RNAs (5S, 16S, 23S) and 62 tRNAs covering all amino acids and pyrrolysine
224 that is encoded by the UAG codon in methylamine methyltransferase genes. 1780
225 hypothetical protein open reading frames accounted for nearly half of all protein features
226 with 1837 putative functional proteins assignments based on similarity to identified
227 protein sequences in public databases. Of hypothetical protein genes conserved at the
228 80% nucleotide level, 289 were shared with *M. acetivorans* and 249 with *M. mazei* of
229 which 105 were common to both and should be considered highly conserved
230 unidentified genes.

231 **Gene Annotation**

232
233 There were 128 unique orfs with sequence identities greater than 67% to genes
234 in the NCBI sequence database but without sequence identity to other methanosarcinal
235 genomes (<http://bigm.umbi.umd.edu/materials/Methanosarcina/>). Some of these
236 features are highlighted below.

237 The *M. barkeri* genome included the full complement of genes encoding
238 enzymes in the hydrogenotrophic, methylotrophic and acetoclastic pathways
239 (Deppenmeier et al. 2002; Galagan et al. 2002). In addition to these a complete
240 formate dehydrogenase operon (MbarA 1561-1562), *fdhAB*, was detected with high
241 sequence identity to catabolic formate dehydrogenase from several formate-utilizing
242 methanogens. *Methanosarcina* spp. have never been reported to utilize formate for
243 growth and *fdhAB* has not been detected previously in this genus (Boone et al. 2001).
244 Attempts to grow *M. barkeri* on 50 mM formate in this study were unsuccessful and the

245 addition of sodium formate to cultures containing trimethylamine or hydrogen did not
246 enhance growth. *M. barkeri* lacks genes encoding a two subunit NDP-forming acetyl-
247 CoA synthetase (*acdAB*) that is found in *M. acetivorans* (MA3168 and MA3602) and *M.*
248 *mazei* (MM0358 and MM0493), but has a remnant of this enzyme, pseudogene
249 MbarA_3662. This enzyme catalyzes one of two pathways for generating acetyl-CoA;
250 the other is the CO dehydrogenase/acetyl-coenzyme A synthase that catalyzes
251 aceticlastic catabolism in *Methanosarcina* spp. The absence of the *acd* genes suggests
252 that the CO dehydrogenase/acetyl-coenzyme A synthase fulfills the function of both
253 enzymes in *M. barkeri*.

254 Among genes encoding biosynthetic functions a group of 14 sequential orfs
255 encode for predicted gas vesicles with highest identity to *GvpAN* (GJKLM) (MbarA326-
256 339) in the haloarchaea, which includes the minimal gene set for expression of vesicle
257 in *Haloflex volcanii* (Offner and Pfeifer 1995). Although there are no reports of gas
258 vesicles in *M. barkeri* Fusaro, gas vesicles have been reported in another strain of
259 *M. barkeri*, FR-1, and in *Methanosarcina vacuolata*, which has 61% homology with the
260 type strain of *M. barkeri* (Archer and King 1984; Zhilina and Zavarzin 1979; Zhilina and
261 Zavarzin 1987). Interestingly, *M. barkeri* has three sequential copies of *GvpA* that
262 encodes the ribs of the vesicle wall and influences the strength and width of the vesicles
263 (Beard et al. 2002). The 33.5 kb region that includes the *Gvp* operon may have been
264 acquired from vesicle synthesizing species as it is flanked by transposons. Gas
265 vesicles are observed occasionally in *M. barkeri* cells grown with H₂-CO₂ on solidified
266 medium. *M. barkeri* also has orfs (MbarA_0022 and MbarA_0023) with high identity to
267 two enzymes required for N-acetylmuramic acid synthesis, which is unique among the

268 sequenced Archaea. However, prior analysis of the cell wall composition of *M. barkeri*
269 Fusaro failed to detect muramic acid (Kandler and Hippe 1977). *M. barkeri* also lacks a
270 low affinity phosphate transporter (MA2935) suggesting it originated in a phosphate-
271 poor environment. Two other transporters are missing in *M. barkeri*, a gluconate
272 transporter (MA0021) and a dicarboxylate transporter (MA2961). This suggests that *M.*
273 *barkeri* may have a lower ability to take up organic compounds than the other two.
274 Finally *M. acetivorans* and *M. mazei* have two copies of cheC (MA0012 and MA3065)
275 but *M. barkeri* does not have this protein. The role of this chemotaxis gene in
276 *Methanosarcina* spp. is currently unknown since motility has not been observed in these
277 species.

278 Another unique feature of the *M. barkeri* genome is the detection of a putative
279 operon encoding a bacterial P450-specific ferredoxin reductase (Mbar 1947-1945). The
280 family of heme protein monooxygenases known as cytochrome P450 plays a critical
281 role in the synthesis and degradation of many xenobiotics and physiologically important
282 compounds (Sono et al. 1966; Sono et al. 1996; Whitlock and Denison 1995). All
283 known P450s are multi-centre enzymes consisting of a heme, or P450, component with
284 associated reductase components. The gene encoding the putative cytochrome P450 in
285 *M. barkeri* is flanked immediately upstream by genes encoding a ferredoxin and
286 ferredoxin reductase, which is typical of bacterial class I three-component systems. For
287 catalytic activity, cytochrome P450 must be associated with the electron donor partner
288 proteins, ferredoxin/ferredoxin reductase complex (Takemori et al. 1993). Cytochrome
289 P450 has not been detected previously in the Archaea. Another putative operon
290 encoding oxygen dependent cytochrome *d* oxidase, *cydAB*, was also identified in the

291 genome of *M. barkeri* and the other two methanosarcinal genomes. The presence of
292 these oxygen dependent genes along with one catalase and two superoxide dismutase
293 suggests that these proteins protect methanosarcinal species from oxygen or they may
294 support microaerophilic growth by a currently undescribed mechanism. As cytochrome
295 P450 catalyzes an oxygen requiring reaction and has not been detected previously in
296 an anaerobe, the detection of this gene in *M. barkeri* raises intriguing questions about
297 the function of this gene product in this obligately anaerobic methanogen.

298 **Plasmid structure and content**

299
300 The 36.4 kb plasmid in *M. barkeri* has not been detected previously. In contrast
301 to the smaller 5.4 kb plasmid pC2A in *M. acetivorans*, which appears to replicate by a
302 rolling-circle mechanism (Metcalf et al. 1997), the *M. barkeri* extrachromosomal element
303 lacks a putative *repA*. Instead it has a *cdc-6* homolog in a region of highly repetitive
304 sequence (discussed below), which suggests a novel mechanism of synchronous
305 replication. Interestingly, one of the extrachromosomal orfs (MbarB 3749) has 44%
306 sequence similarity to an ATPase associated with chromosomal partitioning. These
307 combined characteristics suggest that the extrachromosomal element replicates with
308 cell division. In addition to the putative *cdc6* and partitioning protein, the orfs include 4
309 genes possibly associated with methanochondroitin synthesis, 7 hypothetical genes of
310 unknown function and 5 putative transposases. None of the orfs had equivalent
311 identities to orfs found in *M. acetivorans* and *M. mazei* genomes, but missing from the
312 *M. barkeri* genome that might have suggested a critical function for the
313 extrachromosomal element.

314 **Features revealed by whole genome comparison**

315
316 Whole genome distances (Table 2) based on maximal local alignments indicate
317 that the genomes are quite similar in overall content with *M. acetivorans* and *M. mazei*
318 marginally more closely related. This is in qualitative agreement with DNA-DNA
319 hybridization experiments (Sowers and Johnson 1984), which showed 28% homology
320 between *M. acetivorans* and *M. mazei* and 18% between these species and *M. barkeri*.
321 This result underscores the comparability of these sequences with the exception of the
322 plasmid sequence.

323 **Location of origins of replication**

324
325 In Archaea, origins of replication are invariably found in close proximity to the
326 origin recognition complex gene (*orc1*) sometimes also referred to as cell division
327 control protein 6 (*cdc6*) (Lopez et al. 1999). When genes are densely packed, searches
328 for putative origins of replication are directed at proximal intergenic regions. In the three
329 Methanosarcinae there are two highly conserved paralogous copies of these genes, in
330 relatively close mutual proximity (about 100 kb or 300 kb in *M. barkeri*) situated on
331 opposite strands and directed away from each other, a finding consistent with the
332 observation of Kelman *et al.* (Kelman and Kelman 2004). Flanking downstream ORFs
333 are conserved (Table 3). The putative origins of replication are located in the upstream
334 intergenic regions of approximately 1600 nt (ORI A) or 800 nt (ORI B) in extent and are
335 somewhat conserved at the nucleotide level. In the chromosomal origin of replication
336 region, gene products are approximately 95% identical across all species. Non-coding
337 origin features (ORI A and ORI B) are not as well conserved ($E \leq 1e-44$ in ORI A and

338 E $\leq 1e-8$ in ORI B) and show only weak similarity between ORI A and ORI B. They are
339 extremely AT rich (~70%) and may show unconserved inverted repeat structures.

340 A replication complex is initiated when *orc1* (*cdc6*) protein binds to cognate DNA
341 at the origin and allows the recruitment of MCM and the rest of the replication
342 machinery. An approximate inverted repeat (Figure 3) could allow a pseudo-
343 symmetrical double hairpin to form a crucifix motif similar to a Holliday junction thereby
344 initiating bi-directional replication from a point, with complexes bypassing each other to
345 replicate the origin at the beginning of replication. The concurrent presence of more
346 than one active origin would cause contention for DNA, so there must be an implicit
347 mechanism to control which origin and which origin recognition complex protein is
348 dominant. It is notable that the downstream neighbor of the secondary *orc1* B is a
349 highly conserved hsp60 class heatshock protein as this suggests a possible stress-
350 associated switching mechanism. The putative origins of replication are located
351 centrally within the most highly conserved and syntenous regions of the respective
352 genomes (Figure 4) consistent with the observation of Eisen et al. (Eisen et al. 2000) of
353 symmetrical inversion about the origin of replication. GC skew analysis (results not
354 shown) is not useful in this case as there is a high level of strand inversion and
355 rearrangement.

356 The plasmid of *M. barkeri* presents a unique and distinct origin of replication
357 characterized by an *orc1* homolog (*orc1* C) that is relatively weakly related to *orc1* A
358 and *orc1* B, (37% / 66% with *orc1* A, 21% / 44% with *orc1* B) (Table 3). The
359 immediately adjacent upstream region of the plasmid DNA contains a 5.6 kb non-coding

360 region (15.3% of the plasmid sequence) characterized by highly repetitive sequence
361 consisting of over 38 direct repeats of a 143 nt sequence with few variations between
362 them (Figure S-1, supplement). The consensus of the AT rich repeat sequence is:

363 ATCCCATTTCTTAAGCAGAGAATTAGTTTCCTAAGCAAAAAAAAAAaGATTTCTGgcttagA
364 CCATTTCTTAAGCAAAACGATATCAGAAGACATAACAAGTTAGAAGAaAAAtAAgTT
365 AAAATTAGATATTAATCTGTATATAT, with internal repeats underscored and variable
366 regions in lowercase. This sort of arrangement (ORI C) is quite unlike that of the
367 chromosomal ORI A and ORI B, but has the capacity to present slideable bubbled-out
368 complete repeat motifs and retain a quasi-stable structure (Figure 5).

369

370 **Overall genomic organization**

371 A significant observation in the three-way comparison of the *Methanosarcina*
372 genomes (Figure 4) is the overall collinearity of *M. mazei* and *M. acetivorans* (lower left
373 panel). This attests to a history of conserved gene order and resistance to large scale
374 mosaicity. However closer examination (Figure 6) reveals that there is considerable
375 deviation from the expected 45° slope for a line of identity. This is maintained between
376 *M. barkeri* and *M. mazei*, indicating that *M. acetivorans* has been subject to uniformly
377 distributed local elongation, which may arise from gene duplication, elongation of
378 intergenic regions or insertion of sequence by transposition. This may explain the large
379 size of the *M. acetivorans* genome relative to the other *Methanosarcina* spp.

380 *M. barkeri* is distinguished by having an organization that is well conserved with
381 respect to the other *Methanosarcinae* in the region proximal to the origin of replication
382 where interspecies gene similarities are as high as 95% (Table 3). However there is

383 little apparent conservation of gene organization in the region most distal to the origin
384 where large scale collinearity appears rare. The putative terminus of replication is
385 observed to be a hotspot for reorganization (Myllykallio et al. 2000). Two properties of
386 *M. barkeri* were measured: synteny, which measures the local paralog neighborhood
387 with respect to comparable genomes and intergenic interval or the separation between
388 successive genes which measures the relative content density. In the distal semi-
389 genome the rate of change of synteny is negative in accord with the macroscopic
390 observation of decreased collinearity, and the negatively correlated intergenic interval is
391 greater than average indicating a loss of gene content in this region (Table 2). What
392 might cause this wasteland effect? One possibility, given the symmetry with respect to
393 the origin, is an accumulation of strand exchange failures in the replication process, and
394 subsequent 'gene rot' of broken genes. The cross effect of random strand inversion
395 noted by Eisen et al. (Eisen et al. 2000) gives way to a shotgun effect. Another
396 possibility is infiltration by transposons with transposase mediated damage. Certainly
397 there is an increased frequency of transposon genes in this area (Figure 4, trace d), but
398 this may either be causative or opportunistic, with the organism tolerating infiltration of
399 already dysfunctional sections of the chromosome.

400

401 **CONCLUSIONS**

402

403 Of the 3680 open reading frames in *M. barkeri*, 678 had paralogs with better than
404 80% similarity to both *M. acetivorans* and *M. mazei* while 256 were unique (non-
405 paralogous) amongst these species. An etiology for genome rearrangement is revealed
406 by whole genome comparison of three species of the genus *Methanosarcina*. The

407 inverse correlation of intergenic size and synteny demonstrates a mechanism for the
408 development of genome plasticity, which involves replication associated inversion with
409 concomitant gene damage and colonization by transposon elements. Gene
410 duplication is also observed as a mechanism for genome extension. The organization
411 of *M. barkeri* is well conserved with respect to the other *Methanosarcinae* in the region
412 proximal to the origin of replication with interspecies gene similarities as high as 95%. In
413 the half genome most distant from the origin, it is however disordered and marked by
414 increased transposase frequency and decreased gene synteny and gene density.
415 Furthermore we have observed a highly conserved double origin of replication which
416 suggests a mechanism for replication which allows a double start with pass through
417 which enables the origin itself to be replicated. The apparent genome plasticity likely
418 contributed to these species ability to adapt to a broad range of environments as a
419 result of genome elongation and enrichment for favorable phenotypes.

420

421

422 ACKNOWLEDGEMENTS

423

424

425

426

427

428

429

430

431

432

433

This work was performed under the auspices of the US Department of Energy's Office of Science, Biological and Environmental Research Program and the by the University of California, Lawrence Livermore National Laboratory under Contract No. W-7405-Eng-48, Lawrence Berkeley National Laboratory under contract No. DE-AC03-76SF00098 and Los Alamos National Laboratory under contract No. W-7405-ENG-36. KRS was supported in part by NSF MCB Division of Cellular and Bioscience grant #MCB0110762 and by DOE Energy Biosciences Program grant #DE-FG02-93-ER20106. WWM was supported in part by NSF MCB Division of Cellular and Biosciences grant #MCB12466 and by DOE Energy Biosciences Program grant #DEFG02-02ER15296.

434 **LITERATURE CITED**

435

436 Archer, D.B. and N.R. King. 1984. Isolation of gas vesicles from *Methanosarcina*437 *barkeri*. *J. Gen. Microbiol.* **130**: 167-172.

438 Badger, J.H. and G.J. Olsen. 1999. CRITICA: Coding Region Identification Tool

439 Invoking Comparative Analysis. *Mol. Biol. Evol.* **16**: 512–524.

440 Bateman, A., E. Birney, R. Durbin, S.R. Eddy, K.L. Howe, and E.L. Sonnhammer. 2000.

441 The Pfam protein families database. *Nucleic Acids Research* **28**: 263-266.

442 Beard, S.J., P.K. Hayes, F. Pfeifer, and A.E. Walsby. 2002. The sequence of the major

443 gas vesicle protein, GvpA, influences the width and strength of halobacterial gas

444 vesicles. *FEMS Microbiol. Lett.* **213**: 149-157.

445 Boccazzi, P., K.J. Zhang, and W.W. Metcalf. 2000. Generation of dominant selectable

446 markers for resistance to pseudomonic acid by cloning and mutagenesis of the

447 *ileS* gene from the archaeon *Methanosarcina barkeri* Fusaro. *J. Bacteriol.* **182**:

448 2611-2618.

449 Bomar, M. and K.W. Knoll, F. 1985. Fixation of molecular nitrogen by *Methanosarcina*450 *barkeri*. *FEMS Microbiol. Ecol.* **31**: 47-55.451 Boone, D.R., W.B. Whitman, and Y. Koga. 2001. Genus *Methanosarcina*. In *Bergey's*452 *Manual of Systematic Bacteriology* (eds. D.R. Boone and R.W. Castenholz), pp.

453 268-276. Springer, New York.

454 Conway de Macario, E., D.L. Maeder, and A.J.L. Macario. 2003. Breaking the mould:

455 archaea with all four chaperoning systems. *Biochemical and Biophysical*456 *Research Communications* **301**: 811-812.

- 457 Delcher, A.L., D. Harmon, S. Kasif, O. White, and S.L. Salzberg. 1999. Improved
458 microbial gene identification with GLIMMER. *Nucleic Acids Research* **27**: 4636-
459 4641.
- 460 Deppenmeier, U., A. Johann, T. Hartsch, R. Merkl, R.A. Schmitz, R. Martinez-Arias, A.
461 Henne, A. Wiezer, S. Bäumer, C. Jacobi, H. Brüggemann, T. Lienard, A.
462 Christmann, M. Bömeke, S. Steckel, A. Bhattacharyya, A. Lykidis, R. Overbeek,
463 H.-P. Klenk, R.P. Gunsalus, H.J. Fritz, and G. Gottschalk. 2002. The genome of
464 *Methanosarcina mazei*: Evidence for lateral gene transfer between Bacteria and
465 Archaea. *J. Mol. Microbiol. Biotechnol.* **4**: 453-461.
- 466 Eisen, J., J. Heidelberg, O. White, and S. Salzberg. 2000. Evidence for symmetric
467 chromosomal inversions around the replication origin in bacteria. In *Genome*
468 *Biology*, pp. RESEARCH0011.
- 469 Ewing, B. and P. Green. 1998. Base-calling of automated sequencer traces using
470 phred. II. Error probabilities. *Genome Research* **8**: 186-194.
- 471 Ewing, B., L. Hillier, M.C. Wendl, and P. Green. 1998. Base-calling of automated
472 sequencer traces using phred. I. Accuracy assessment. *Genome Research* **8**:
473 175-185.
- 474 Galagan, J.E., C. Nusbaum, A. Roy, M.G. Endrizzi, P. Macdonald, W. FitzHugh, S.
475 Calvo, R. Engels, S. Smirnov, D. Atnoor, A. Brown, N. Allen, J. Naylor, N.
476 Stange-Thomann, K. DeArellano, R. Johnson, L. Linton, P. McEwan, K.
477 McKernan, J. Talamas, A. Tirrell, W.J. Ye, A. Zimmer, R.D. Barber, I. Cann, D.E.
478 Graham, D.A. Grahame, A.M. Guss, R. Hedderich, C. Ingram-Smith, H.C.
479 Kuettner, J.A. Krzycki, J.A. Leigh, W.X. Li, J.F. Liu, B. Mukhopadhyay, J.N.

- 480 Reeve, K. Smith, T.A. Springer, L.A. Umayam, O. White, R.H. White, E.C. de
481 Macario, J.G. Ferry, K.F. Jarrell, H. Jing, A.J.L. Macario, I. Paulsen, M. Pritchett,
482 K.R. Sowers, R.V. Swanson, S.H. Zinder, E. Lander, W.W. Metcalf, and B.
483 Birren. 2002. The genome of *Methanosarcina acetivorans* reveals extensive
484 metabolic and physiological diversity. *Genome Research* **12**: 532-542.
- 485 Gordon, D., C. Abajian, and P. Green. 1998. Consed: a graphical tool for sequence
486 finishing. *Genome Research* **8**: 195-202.
- 487 Grigoriev, A. 1998. Analyzing genomes with cumulative skew diagrams. *Nucleic Acids*
488 *Research* **26**: 2286–2290. .
- 489 Kandler, O. and H. Hippe. 1977. Lack of peptidoglycan in the cell walls of
490 *Methanosarcina barkeri*. *Arch. Microbiol.* **113**: 57-60.
- 491 Kelmana, L.M. and Z. Kelman. 2004. Multiple origins of replication in archaea *Trends in*
492 *Microbiology* **12** 399-430.
- 493 Kreisl, P. and O. Kandler. 1986. Chemical structure of the cell wall polymer
494 methanosarcina. *Syst. Appl. Microbiol.* **7**: 293-299.
- 495 Lobo, A.L. and S.H. Zinder. 1988. Diazotrophy and Nitrogenase Activity in the
496 Archaeobacterium *Methanosarcina barkeri* 227. *Appl. Environ. Microbiol.* **54**:
497 1656-1661.
- 498 Lopez, P., H. Philippe, H. Myllykallio, and P. Forterre. 1999. Identification of putative
499 chromosomal origins of replication in Archaea. *Molecular Microbiology* **32**: 883-
500 886.
- 501 Lovley, D.R. and M.J. Klug. 1982. Intermediary metabolism of organic matter in the
502 sediments of a eutrophic lake. *Appl. Environ. Microbiol.* **43**: 552-560.

- 503 Markowitz, V., F. Korzeniewski, K. Palaniappan, E. Szeto, G. Werner, A. Padki, X.
504 Zhao, I. Dubchak, P. Hugenholtz, I. Anderson, A. Lykidis, K. Mavromatis, N.
505 Ivanova, and N.C. Kyrpides. 2006. The Integrated Microbial Genomes (IMG)
506 System. *Nucleic Acids Research (special database issue)* **34**: D344-348.
- 507 Metcalf, W.W., J.K. Zhang, E. Apolinario, K.R. Sowers, and R.S. Wolfe. 1997. A genetic
508 system for Archaea of the genus *Methanosarcina*: Liposome-mediated
509 transformation and construction of shuttle vectors. *Proc Natl Acad Sci USA* **94**:
510 2626-2631.
- 511 Metcalf, W.W., J.K. Zhang, X. Shi, and R.S. Wolfe. 1996. Molecular, genetic, and
512 biochemical characterization of the serC gene of *Methanosarcina barkeri* fusaro.
513 *J Bacteriol* **178**: 5797-5802.
- 514 Mulder, N.J., R. Apweiler, T.K. Attwood, A. Bairoch, A. Bateman, D. Binns, P. Bradley,
515 P. Bork, P. Bucher, L. Cerutti, and e. al. 2005. InterPro, progress and status in
516 2005. *Nucleic Acids Research* **33**: D201–D205.
- 517 Myllykallio, H., P. Lopez, P. Lopez-Garcia, R. Heilig, W. Saurin, Y. Zivanovic, H.
518 Philippe, and P. Forterre. 2000. Bacterial Mode of Replication with Eukaryotic-
519 Like Machinery in a Hyperthermophilic Archaeon. *Science* **288**: 2212-2215.
- 520 Offner, S. and F. Pfeifer. 1995. Complementation studies with the gas vesicle-encoding
521 p-vac region of *Halobacterium salinarium* PHH1 reveal a regulatory role for the
522 p-gvpDE genes. *Mol. Microbiol.* **16**: 9-19.
- 523 Rother, M. and W.W. Metcalf. 2004. Anaerobic growth of *Methanosarcina acetivorans*
524 C2A on carbon monoxide: An unusual way of life for a methanogenic archaeon.

- 525 *Proceedings of the National Academy of Sciences of the United States of*
526 *America* **101**: 16929-16934.
- 527 Rother, M. and W.W. Metcalf. 2005. Genetic technologies for Archaea. *Curr Opin*
528 *Microbiol* **8**: 745-751.
- 529 Sono, M., M.P. Roach, E.D. Coulter, and J.H. Dawson. 1966. *Chem.Rev.* **96**: 2841-
530 2887.
- 531 Sono, M., M.P. Roach, E.D. Coulter, and J.H. Dawson. 1996. Heme-containing
532 oxygenases. *Chem. Rev.* **96**: 2841-2887.
- 533 Sowers, K.R. 1995. Growth of *Methanosarcina* spp. as single cells. In *Archaea: A*
534 *Laboratory Manual* (eds. F.T. Robb K.R. Sowers S. DasSharma A.R. Place H.J.
535 Schreier, and E.M. Fleischmann), pp. 61-62. Cold Spring Harbor Laboratory
536 Press, Cold Spring Harbor.
- 537 Sowers, K.R. 2004. Methanogenesis. In *The Desk Encyclopedia of Microbiology* (ed. M.
538 Schaechter), pp. 659-679. Elsevier Academic Press, San Diego.
- 539 Sowers, K.R., J.E. Boone, and R.P. Gunsalus. 1993. Disaggregation of *Methanosarcina*
540 spp. and growth as single cells at elevated osmolarity. *Appl. Environ. Microbiol.*
541 **59**: 3832-3839.
- 542 Sowers, K.R. and J.G. Ferry. 1983. Isolation and characterization of a methylotrophic
543 marine methanogen, *Methanococcoides methylutens* gen. nov., sp. nov. *Appl.*
544 *Environ. Microbiol.* **45**: 684-690.
- 545 Sowers, K.R. and J.L.F. Johnson, J. G. 1984. Phylogenetic relationships among the
546 methylotrophic methane-producing bacteria and emendation of the
547 family *Methanosarcinaceae*. *Int. J. Syst. Bacteriol.* **34**: 444-450.

- 548 Takemori, S., T. Yamazaki, and S. Ikushiro. 1993. Evolution and differentiation of P450
549 genes. In *Cytochrome P450* (ed. T. Omura, Ishimura, Y., and Fujii-Kuriyama, Y.).
550 VCH Publishers, Inc., New York.
- 551 Tatusov, R.L., N.D. Fedorova, J.D. Jackson, A.R. Jacobs, B. Kiryutin, E.V. Koonin, D.M.
552 Krylov, R. Mazumder, S.L. Mekhedov, A.N. Nikolskaya, and e. al. 2003. The
553 COG database: an updated version includes eukaryotes. *BMC Bioinformatics* **4**:
554 41.
- 555 Welander, P.V. and W.W. Metcalf. 2005. Loss of the mtr operon in *Methanosarcina*
556 blocks growth on methanol, but not methanogenesis, and reveals an unknown
557 methanogenic pathway. *PNAS* **102**: 10664-10669.
- 558 Whitlock, J.P.J. and M.S. Denison. 1995. In dusction of cytochrome P450 enzyme that
559 metabolize xenobiotics. In *Cytochrome P450: Structure, Mechanisms and*
560 *Biochemistry* (ed. P.R. Ortiz de Montellano), pp. 367-390. Plenum Press, New
561 York.
- 562 Zhilina, T.N. and G.A. Zavarzin. 1979. Comparative cytology of methanosarcinae and
563 description of *Methanosarcina vacuolata* sp. nova. *Microbiology* **48**: 279-285.
- 564 Zhilina, T.N. and G.A. Zavarzin. 1987. *Methanosarcina vacuolata* sp. nov., a vacuolated
565 *Methanosarcina*. *Int. J. Syst. Bacteriol.* **37**: 281-283.
- 566

567
568
569
570
571

Table 1. Comparison of Genome Features Among *Methanosarcina* spp.

Organism	<i>Methanosarcina acetivorans</i>	<i>Methanosarcina mazei</i>	<i>Methanosarcina barkeri fusaro</i>	<i>Methanosarcina barkeri fusaro</i>	<i>Methanosarcina barkeri fusaro</i>
tax_id	188937	192952	269797	269797	269797
Accession	NC_003552	NC_003901	NC_007355	NC_007349	
designation	chromosome	chromosome	chromosome	plasmid	genome
length	5751494	4096345	4837408	36358	4873766
G+C%	42.7%	41.5%	39.2%	33.6%	39.2%
feature count	4540	3371	3680	18	3698
features length	4262934	3074712	3390164	21099	3411263
features coverage	74%	75%	70%	58%	69%
featureless nt/feature mean	26%	25%	30%	42%	31%
	939	912	921	1172	922

572

573 **Table 2.** Intergenomic distances calculated using eq 1 based on whole genome
 574 maximal local nucleotide sequence identity considering only HSPs with identity > 67%
 575 (lower left) or 55% (upper right).

576

	<i>M. acetivorans</i>	<i>M. mazei</i>	<i>M. barkeri</i>	<i>M. barkeri</i> plasmid
<i>M. acetivorans</i>	0	0.489	0.487	0.570
<i>M. mazei</i>	0.517	0	0.480	0.591
<i>M. barkeri</i>	0.552	0.569	0	0.512
<i>M. barkeri</i> plasmid	0.881	0.883	0.836	0

577

578

579

580

581

582

583

Table 3. Identification of conserved features for chromosomal origins of replication in *Methanosarcina* spp.

Description	strand	<i>M. acetivorans</i>	<i>M. barkeri</i>	<i>M. mazei</i>
conserved hypothetical	+	GI:20093437	GI:73668510	GI:21227413
conserved hypothetical	+	GI:20093438	GI:73668511	GI:21227414
conserved hypothetical	+	GI:20093439	GI:73668512	GI:21227415
orc1 A	-	GI:20088900	GI:73668513	GI:21227416
ORI A		1529 - 3357	1189197 - 1191361	1564667 - 1566241
inter-origin region	variable	~100Kbp	~300Kbp	~100Kbp
conserved hypothetical	-	GI:20088912	GI:73668731	GI:21227479
ORI B		104571 - 105272	1481179 - 1482170	1654267 - 1655075
orc1 B	+	GI:20088912	GI:73668732	GI:21227480
Hsp60	-	GI:20088912	GI:73668733	GI:21227481

584

585 **FIGURE LEGENDS**

586

587 **Figure 1.** Thin-section electron micrograph of *M. barkeri* Fusaro showing typical
588 morphology consisting of multicellular aggregates embedded in a methanochondroitin
589 matrix. Vacuole-like structures appear to be membrane bound. Bars: A, 1.0 μm , B, 0.2
590 μm .

591

592 **Figure 2.** GRIT database schema. Primary keys are capitalized, foreign keys are
593 underlined. Arrows indicate foreign key primary key relationships

594

595 **Figure 3.** The *M. barkeri* ORI A self-complementary region blastn alignment.

596

597 **Figure 4.** Asymmetric fragmentation in *M. barkeri*. The top panel shows cumulative
598 deviations from the mean in *M. barkeri* genome for synteny (SI) with respect to
599 *M. acetivorans* (a), *M. mazei* (b), or intergenic interval (c). The cumulative transposon
600 count is superimposed (d). The bottom panel shows uniformly scaled blastn cross plots
601 of *M. barkeri* chromosome with *M. mazei* and *M. acetivorans* with the origin regions
602 circled.

603

604 **Figure 5.** Proposed mechanism for conserved repetitive sequence to provide bubbled-
605 out repeat motifs for initiation of replication. Pairs of quasi-stable bubbles might occur in
606 pairs at arbitrary locations on opposite strands. All motifs are essentially identical.

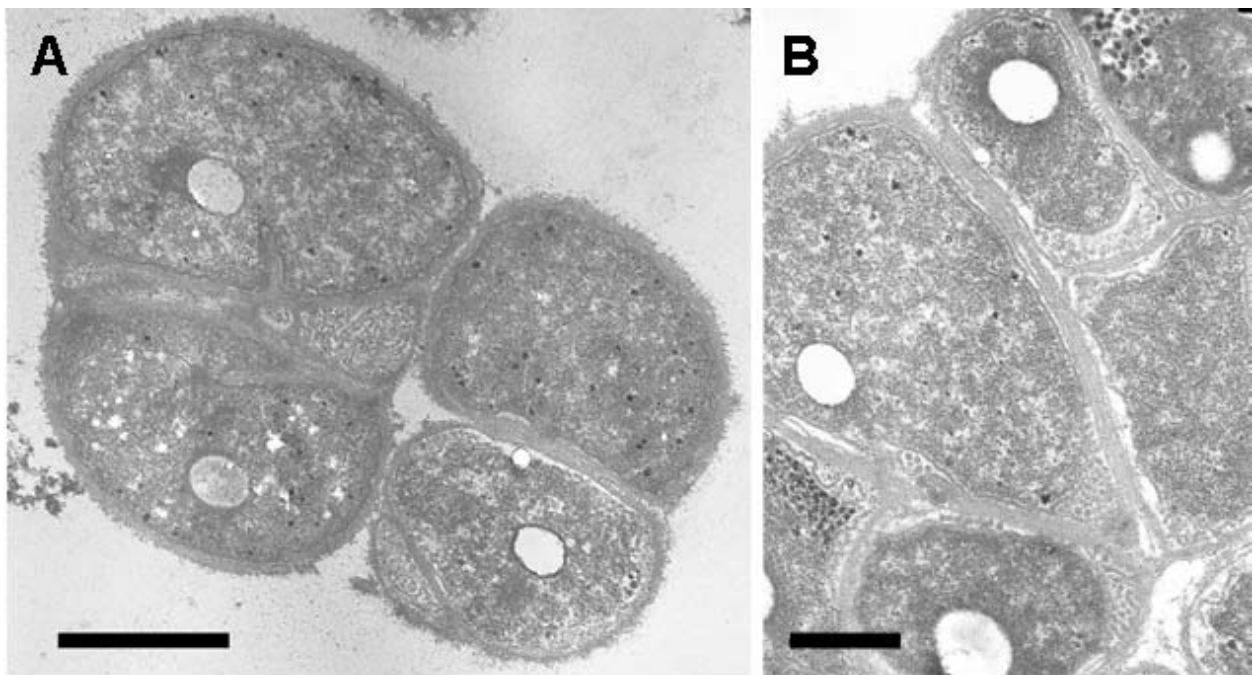
607

608 **Figure 6.** *M. acetivorans* is elongated due to distributed gene duplication events.

609 **Figure 1.** Thin-section electron micrograph of *M. barkeri* Fusaro showing typical
610 morphology consisting of multicellular aggregates embedded in a methanochondroitin
611 matrix. Vacuole-like structures appear to be membrane bound. Bars: A, 1.0 μm , B, 0.2
612 μm .

613

614



615

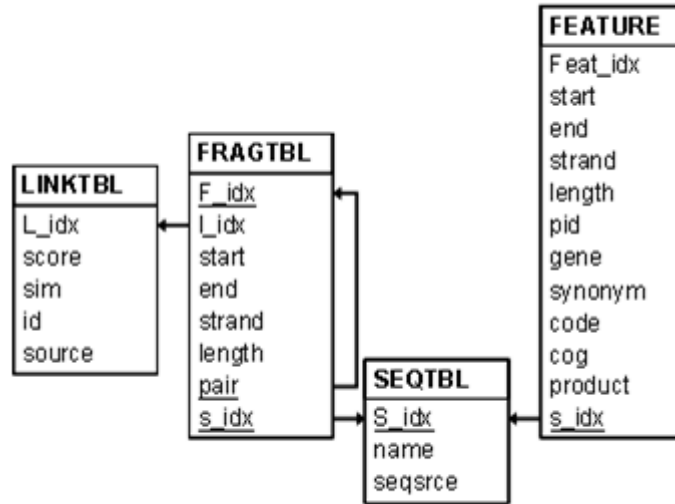
616

617

618

619

620 **Figure 2.** GRIT database schema. Primary keys are capitalized, foreign keys are
 621 underlined. Arrows indicate foreign key primary key relationships.
 622
 623
 624
 625
 626
 627
 628
 629
 630
 631
 632
 633
 634
 635
 636
 637



638 **Figure 3.** The *M. barkeri* ORI A self-complementary region blastn alignment

639
640
641
642
643
644
645
646
647
648
649
650
651
652
653
654
655
656
657
658
659
660
661
662
663
664
665
666
667
668
669
670

```

Query:      709 CAGAAAATGTAA-ATTTCTCAGAAC-A-TGTAATTTAGATTTCT-CAATTT-TTT-GAAA 656
              || ||||| || | ||| ||||| || |||| ||||| || |||| ||||| || |||| |||||
Sbjct: 1190360 CAAAAAAT-TATGAGTTC-CAGAACCAATGTAGGTTAAATTTAAACCCTTTCTTTTCGAAT 1190417

Query:      655 ATCATACTTTTTCTGA-T-AGATTGAGTATCA-ATAAAAACTCAAAATAAAAAATATTCAA 599
              ||| ||| | | | | | | | | | | | | | | | | | | | | | | | | | | | | | |
Sbjct: 1190418 GGAATAAGTTATGAAAATTATAAT-ATTTTTACATAAAATTTAAAAATAAAAAATTTT-AA 1190475

Query:      598 TGAAAATATTA-AATCA 583
              || | | |||| | | | |
Sbjct: 1190476 -GATAAAATTAGAATTA 1190491

              -- Unaligned region of ~440 nt --

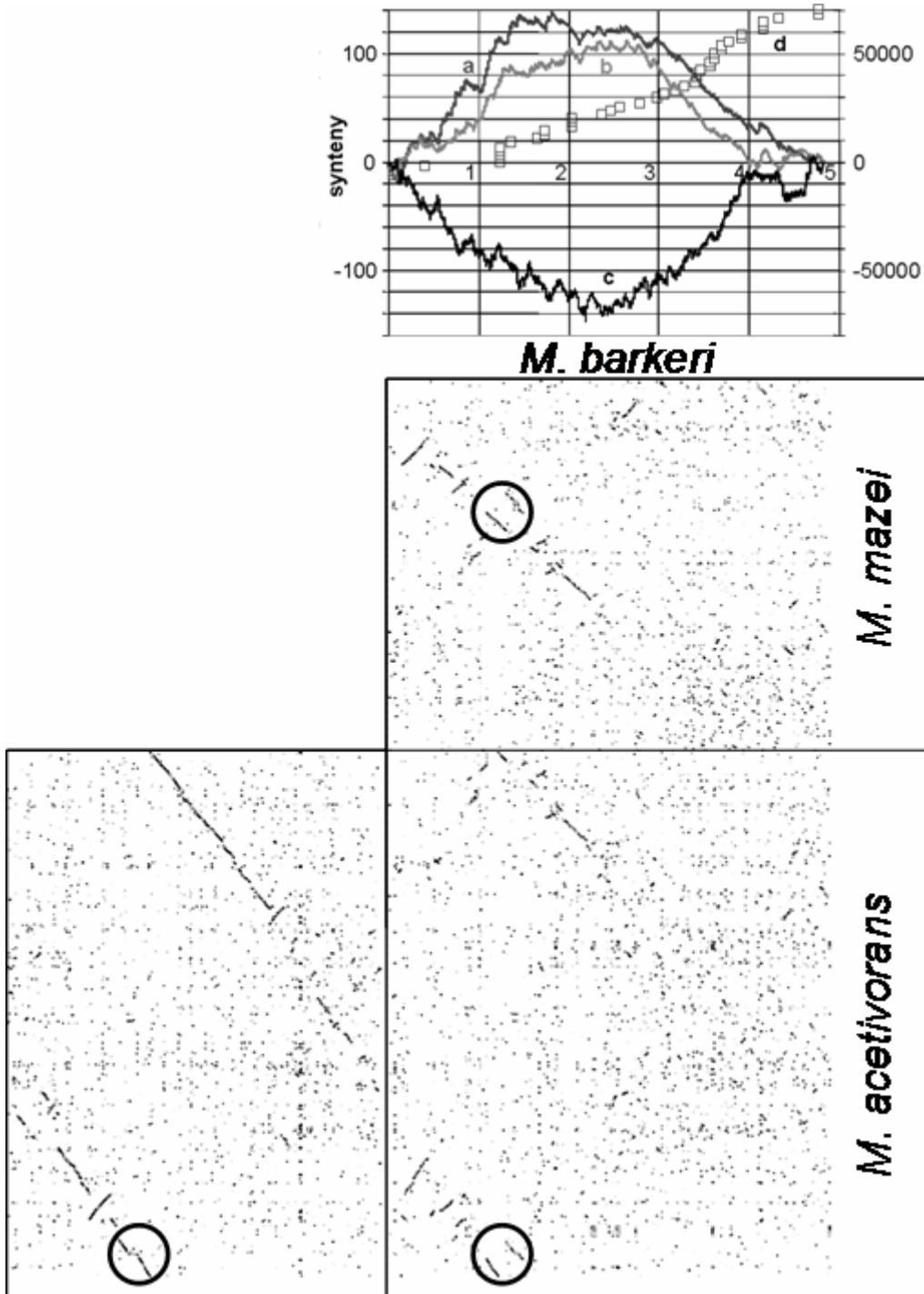
Query:      141 TAATTCTAATTTTATC-TTAAA-ATTTTATTTTTTAATTTTATGTAAAAAT-ATTATAA 85
              | ||| |||| | | | | | | | | | | | | | | | | | | | | | | | | | | | | | |
Sbjct: 1190933 TGATT-TAATATTTTCATTGAATATTTTATTTTGAGTTTTTAT-TGATACTCAATCTA- 1190989

Query:      84 TTTTCATAACTTATTCCATTCGAAAGAAAGGGTTTAAATTTAACCTACATTGGTTCTG-G 26
              | | | | | | | | | | | | | | | | | | | | | | | | | | | | | | | | | | |
Sbjct: 1190990 TCAGAAAAGT-ATGATTTTC-AAA-AAATTGAG-AAATCTAAATTACAT-G-TTCTGAG 1191043

Query:      25 AACTCATA-ATTTTTTG 10
              || | || ||||| || |
Sbjct: 1191044 AAATT-TACATTTTCTG 1191059
    
```

671
672
673
674
675
676
677
678

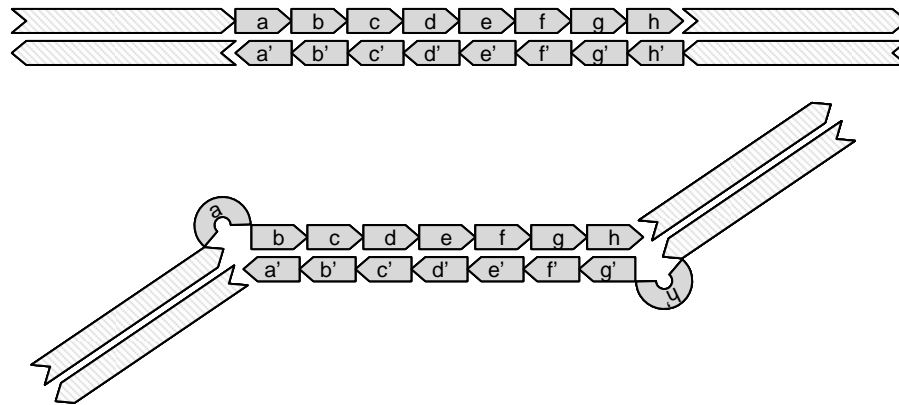
Figure 4. Asymmetric fragmentation in *M. barkeri*. The top panel shows cumulative deviations from the mean in *M. barkeri* genome for synteny (SI) with respect to *M. acetivorans* (a), *M. mazei* (b), or intergenic interval (c). The cumulative transposon count is superimposed (d). The bottom panel shows uniformly scaled blastn cross plots of *M. barkeri* chromosome with *M. mazei* and *M. acetivorans* with the origin regions circled.



679

680
681
682
683
684
685
686
687

Figure 5. Proposed mechanism for conserved repetitive sequence to provide bubbled-out repeat motifs for initiation of replication. Pairs of quasi-stable bubbles might occur in pairs at arbitrary locations on opposite strands. All motifs are nearly identical.



688
689
690
692
694

Figure 6. *M. acetivorans* is elongated due to distributed gene duplication events.

